Available online at www.sciencedirect.com
SCIENCE DIRECT®
ELSEVIER
International Journal of Solids and Structures 41 (2004) 6631–6646
INTERNATIONAL JOURNAL OF SOLIDS and STRUCTURES
www.elsevier.com/locate/ijsolstr

Non-linear and failure behaviour of spotwelds: a "global" finite element and experiments in pure and mixed modes I/II

Bertrand Langrand [a,*], Alain Combescure [b,1]

[a] Department of Solid and Damage Mechanics, ONERA-Lille, 5, boulevard Paul Painlevé, F-59045 Lille Cedex, France
[b] LaMCoS, INSA-Lyon, 18-20, allée des sciences, F-69621 Villeurbanne Cedex, France

Received 7 June 2004
Available online 20 July 2004

Abstract

The paper deals with joint element model used in crashworthiness simulations. The first part of the paper is dedicated to the formulation of a new "global" finite element for spotweld modelling. The mechanical behaviour of the joint is elastic–plastic type and damage is taken into account to model the failure of the welded area. The second part of the paper concerns a new experimental procedure for joint strength analysis in pure and mixed modes I/II and for joint model characterisation. Experiment is based on Arcan principle and results are compared to open literature. In the last part of the paper, the parameters of the new joint model are identified using experiments and used for several shapes of spot-welded specimens. The model predicts reasonably the elastic–plastic part of the response but is unable to predict the post-peak response observed especially in the case of pure shear.

Keywords: Spotweld; Experiment; Equivalent model; Crashworthiness; Damage

1. Introduction

For public transport, safety requirements are growing even when manufacturers want to reduce the design period by using more and more finite element (FE) simulations instead of experiments. Today, the size of FE models used to study crashworthiness may be expressed in terms of 10^5 shell elements (e.g. 10^5 for a car, 2×10^5 for a commercial aircraft such as A320 and 5×10^5 for a train). This huge number of elements is required to model the geometry of frameworks and to describe non-linear behaviours and failure modes. There are of course tens thousand assemblies to joint the parts of the framework (e.g. rivet,

* Corresponding author. Tel.: +33-03-20-49-69-79; fax: +33-03-20-52-95-93.
E-mail addresses: bertrand.langrand@onera.fr (B. Langrand), alain.combescure@insa-lyon.fr (A. Combescure).
[1] Tel.: +33-04-72-43-64-26; fax: +33-04-78-89-09-80.

0020-7683/$ - see front matter © 2004 Elsevier Ltd. All rights reserved.
doi:10.1016/j.ijsolstr.2004.06.009

Nomenclature

a and b parameters for coupling in the engineering failure criterion
A, B and n parameters of the Ludwik material law
A_y and A_z joint parameters for shear behaviour
α angular position of the Arcan set-up
B_y and B_z joint parameters for bending
$\delta(F_m)$ maximum force corresponding displacement
δ_u displacement at failure
D_c critical damage
E_t total absorbed energy
E_1 energy absorbed before the peak of load
E_2 energy absorbed after the peak of load
F_m maximum force
F_y yield force
N, $\overline{N}$ and N_u current, normalized and ultimate normal (tensile) forces
T, $\overline{T}$ and T_u current, normalized and ultimate tangential (shear) forces
P_s and P_u joint parameters for failure
V_{imp} imposed velocity

spotweld). The calculation cost of such models is about hundred hours for a supercomputer until the ultimate failure of the framework appears.

In crash analysis, one usually represents thin structures by shell elements such as MITC4 elements (Dvorkin and Bathe, 1984) or, more likely for explicit codes, under integrated elements like Belytschko and Tsai (1983) or QPPS (Zeng and Combescure, 1998) assumed-strain quadrilateral elements. The weld is represented by a single beam attached to two points located anywhere within the finite elements.

The paper presents the basis of a new equivalent joint element recently implemented within Radioss FE code (1998). The second part of the paper deals with experiments dedicated to joint strength analysis. The parameters of the joint equivalent model are identified and finally evaluated for several specimen shapes. A first attempt to identify the model on more global experiments was presented by Combescure et al. (2003).

2. Equivalent joint model

The welded region is a very complex zone for which the geometry is not very well-known, the actual material properties are complex and highly variable from point to point. We shall ignore these details and replace the whole "welded zone" by a single non-linear spring which represents the "homogenised" behaviour of the region. The non-linear response will be considered elastic–plastic. We will also introduce a damage model in order to be able to simulate the failure of the welded region.

2.1. Linear elastic model

The beam element is a two nodes straight beam with six degrees of freedom per node: three translations w_1, w_2, w_3 and three rotations $\theta_1, \theta_2, \theta_3$ (these quantities are expressed in the local frame of the beam, the direction 3 being the main direction of the beam). The stiffness matrix is derived directly from the following expression of the elastic strain energy:

$$2W^{\text{def}} = ESL\varepsilon_{33}^2 + EI(\chi_1^2 + \chi_2^2) + GJ\psi^2 + 4GS_{\text{R}}(\varepsilon_{13}^2 + \varepsilon_{23}^2) \tag{1}$$

In Eq. (1) E, S, L, I, J, G are respectively the Young's modulus, the section, the length, the bending inertia, the torsion inertia, and the shear modulus. The reduced shear modulus GS_{R} is defined by Eq. (2).

$$GS_{\text{R}} = \frac{1}{\frac{1}{GS} + \frac{L^2}{12EI}} \tag{2}$$

The strains are defined in the following Eq. (3):

$$\begin{cases} \varepsilon_{33} = w_3' - x_1\theta_2' + x_2\theta_1' \\ 2\varepsilon_{13} = w_1' - x_2\theta_3' + \theta_2 \\ 2\varepsilon_{23} = w_2' + x_1\theta_3' + \theta_1 \end{cases} \tag{3}$$

In practice, since the geometry is not known very well, the global elastic stiffness is fitted comparing the model with the observed linear experimental response.

2.2. Plastic model

We will now assume the behaviour of the link to be elastic–plastic. The dual variable consists of one normal force N_3, the two shear forces (N_1, N_2), two bending moments (M_1, M_2) and one torsion moment M_3. We then use a quadratic yield surface F shape and we assume that the generalized stresses are uncoupled in order to predict yielding:

$$F(p) = \left(\frac{N_3}{N_0}\right)^2 + 3a_1^2\left(\frac{N_1}{N_0}\right)^2 + 3a_2^2\left(\frac{N_2}{N_0}\right)^2 + b_1^2\left(\frac{M_1}{M_0}\right)^2 + b_2^2\left(\frac{M_2}{M_0}\right)^2 + c\left(\frac{M_3}{M_0}\right)^2 - \beta^2(p) \tag{4}$$

Parameter p represents the cumulated equivalent plastic strain. Parameters a_i are chosen to fit the plastic behaviour under shear loading; the b_i are used to fit the bending behaviour and parameter c controls the torsional yield stress. Function $\beta(p)$ is used to represent the material's hardening curve. For a perfectly plastic material, we have simply $\beta(p) = 1$. This is an Ilyushin-type model (1956). The treatment of hardening was introduced, for instance, by Chapuliot and Combescure (1993). The reference normal stress N_0 is simply the normal load for which the section yields. The reference bending moment M_0 can be is the moment for which the section starts to plastify when submitted to pure bending. Let us observe that the model is based on a material stress/strain curve represented by the $\beta(p)$ function. The plastic strains are calculated simply by using an associated flow rule. The main interest of the proposed model is that it couples the loads in different directions (e.g. one bending load combined with one tensile or shear force). This is in good agreement with the observed experimental results.

The proposed model omits the strain rate effects. The strain rate dependency can be added to this model introducing the rate effects (e.g. Johnson Cook model). It consists simply to have a material stress strain curve depending of the strain rate ($\beta(p, \dot{p})$).

2.3. Damage and failure

The damage model is simply the ductile failure model (Lemaitre and Chaboche, 1985): we introduce a damage variable denoted D. When damage reaches some critical value denoted D_{c} the material fails. This model is represented by an evolution of the Young's modulus as follows:

$$\begin{cases} E(D) = E(1-D) \\ \dot{D} = 0 \quad \text{if } \dot{p} = 0 \\ \dot{D} = 0 \quad \text{if } p < p_s \text{ or } N_3 < 0 \\ \dot{D} = \frac{D_c}{p_u - p_s}\dot{p} \quad \text{if } \dot{p} \neq 0 \end{cases} \tag{5}$$

Damage increases linearly with the cumulated plastic strain p. This model is totally uncoupled.

3. Experiments for characterisation joint models

The joints control the deformation modes of a framework, but the size of structural crashworthiness problems as well as the number of joints does not allow the model joints using refined local finite element meshes. For such structural-oriented problems, the joints are usually modelled using independent equivalent elastic–plastic elements as presented before. The mechanical behaviours (elastic, plastic and damage) of the joint element are identified independently on tests which are supposed to be only in one "direction" of loading.

Let us now consider a commonly used engineering failure criterion defined by Eq. (6) usually implemented in explicit FE codes such as Radioss. Other criterions more physics-based combined yield function was proposed recently by Lin et al. (2003).

$$(N/N_u)^a + (T/T_u)^b = 1 \tag{6}$$

Let us first quote that Eq. (6) is very similar to Eq. (4) chosen for our model: we have supposed that $a = b = 2$, $N_u = N_0$ and $T_u = N_0/\sqrt{3a_1}$. Pull-out tensile (or coach-peel) tests are performed to characterise the parameter N_u and shear single lap tests (with clamping system) for the parameter T_u. Both parameters are identified to be the maximum force. To identify the parameters a and b, it is necessary to perform at least two mixed tensile/shear tests (such as a shear single lap test but without clamping systems). A lot of authors has assumed $a = b$ because of a lack in experiments (Markiewicz et al., 2001).

The metal plates of the specimens are usually plastically deformed in such experiments. If the failure properties of the joint may be defined easily, its non-linear hardening cannot be extracted easily from the experiments. Some authors have tried inverse methods to characterise the non-linear behaviour of the equivalent joint elements but coarse meshes FE models (the size of the shell element is adapted to structural calculation) hardly succeeded in correlating the experimental deformed shapes of the specimens (Markiewicz et al., 2001). Moreover, as shown recently by Lin et al. (2003) tensile loads include uniaxial or biaxial tension modes and the maximum load may differ by 41%. In this paper we propose a solution to improve the experimental procedure in order to derive directly mechanical properties of joint equivalent models used in crashworthiness analysis.

3.1. Pure and mixed tensile/shear loads devices

Experimental procedures have been developed to test a specimen in pure tension (mode I) and pure shear (mode II) loads and in mixed mode I/II loads (e.g. Arcan et al., 1978; Voloshin and Arcan, 1980; Iosipescu, 1967 or d'Almeida and Monteiro, 1999). The Arcan test was firstly developed to study and characterise the damage behaviour of composite materials (Arcan et al., 1978; Voloshin and Arcan, 1980). Other problems such as crack propagation in metal plates have been studied with this type of tests (Sutton et al., 2000a,b). This experimental set-up enables one to mix and control tensile and shear loads (Fig. 1). The angular position, α, between the two disk quarters and the load direction, defines exactly the tensile/shear ratio. Varying this angular position leads to several load combinations. The global load F is applied to the centre

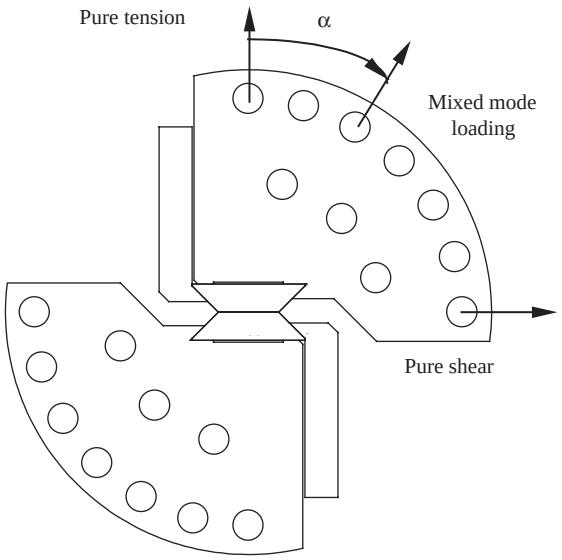

Fig. 1. Arcan device.

of the specimen and may be split into two components (N for local tensile load and T for local shear load) as a function of the angular position α with relations (7).

$$N(\alpha) = F \cdot \cos(\alpha) \quad \text{and} \quad T(\alpha) = F \cdot \sin(\alpha) \tag{7}$$

As proposed by Lin et al. (2002), normalized opening and shear loads may be defined to rule out the effects of the yield stresses for several materials or of the diameter of several spotwelds (8) and (9).

$$\overline{F} = F / \max(F(0°)) \tag{8}$$

$$\overline{N}(\alpha) = \overline{F} \cdot \cos(\alpha) \quad \text{and} \quad \overline{T}(\alpha) = \overline{F} \cdot \sin(\alpha) \tag{9}$$

Patronelli et al. (1999) and Langrand et al. (2000) have developed this experimental set-up to characterise the mechanical properties of riveted joints for quasi-static pure and mixed tensile/shear loading. The engineering failure criterion (6) defined with the experimental results has improved the failure prediction of airframe sub-structure calculations (Langrand et al., 2001). The experimental procedures have been recently adapted by Langrand and Fabis (2002) to high velocity testing in order to assess the strain rate sensitivity of riveted joint in pure and mixed tensile/shear loads.

In the case of spotwelds, the behaviour of the assembly is a function of the welded point and of the metal plate as well. Local strains around the welded point in the plate contribute locally to the observed non-linear behaviour of the assembly. It is then necessary to integrate the local strains within a certain volume of metal plate in the behaviour of the equivalent joint element. These local strains will be filtered anyway by the size of the shell element used in structural calculation (fine at the structure level but too coarse at the joint level). Lee et al. (1998) and Riesner et al. (2000) have proposed an adaptation of the Arcan type test to spotweld by using U shape specimens (Fig. 2). More recently, Hanseen and Langseth (2003) have tried that kind of device for self-pierce rivets but the failure criterion (6) identified with an inverse approach does not succeeded in predicting the behaviour of a structural component. In fact, these devices enable to characterise the mechanical strength of the joint in terms of forces, but not the non-linear behaviour to be used in FE equivalent joint model. Lin et al. (2002) proposes another solution with a more elaborated square cup

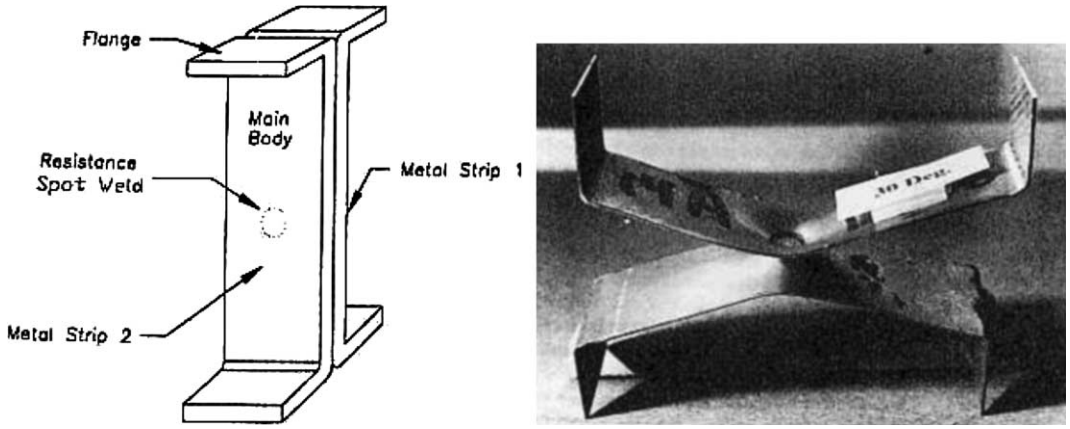

Fig. 2. U shape specimens for Arcan type device from Lee et al. (1998).

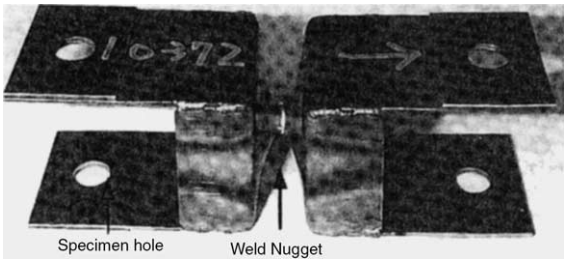

Fig. 3. Square cup specimens for Arcan type device from Lin et al. (2002).

specimen (Fig. 3). For pure opening mode the specimen square profile is not in favour of isotropic strain fields around the welded point. Computations have however shown that the K field was within 1% of the average K around the nugget circumference for small strains (Wang et al., submitted for publication). For large strains experimental observations suggest a relative uniform plastic deformation near the nugget circumference in the cup specimen (Lin et al., 2003). However, the experimental set-up does not provided results for pure shear loading conditions.

To make up for these problems and apply 'properly' the Arcan test principle to spotweld characterisation (for crashworthiness equivalent joint element purpose), the authors propose the solution shown in Fig. 4. The specimen is made of heels and spot-welded plates. The specimen is completely integrated in an

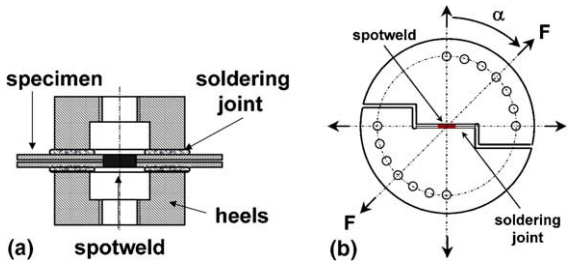

Fig. 4. Soldered specimens for Arcan type device: (a) specimen, (b) device.

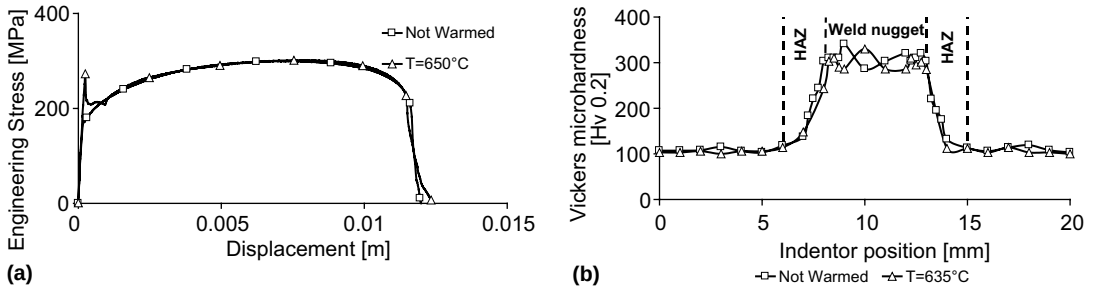

Fig. 5. Influence of the melting temperature of the soldering joint: (a) base metal material law, (b) spotweld microhardness.

Arcan type device (Fig. 4). The aim is to limit and control the deformation of the metal plates, to simplify as much as possible the experimental set-up, and to control the experimental boundary conditions for FE modelling and numerical optimisation reasons. A soldering joint is implemented to link the spot-welded plates and the heels.

Experiments have been performed regarding the mechanical strength of soldering joint using lead/tin or silver/tin alloys. Results have shown that the lead/tin alloy was not tough enough for the considered spotwelds (diameter of the spotweld: 6 mm, base metal: XES mid-steel and thickness of the metal plates: 1.2 mm). The problem in using the silver/tin alloys was the melting temperature of the soldering joint (about 635 °C). So the influence of this melting temperature has been investigated about the constitutive law for the base metal of the plates, and the mechanical strength and the Vickers microhardness diagram for the spotweld. No influence of the melting temperature has been measured on the behaviour of welded point or the base metal properties (Fig. 5). A vacuum furnace has been used to perform the soldering joint in order to avoid oxidation phenomena at the interface between the heels and the spot-welded plates.

3.2. Experimental results

The Arcan test procedure developed for spotwelds is shown in Fig. 6. The base material for specimens is XES steel with the following mechanical properties: yield stress $\sigma_y = 171$ MPa and ultimate tensile stress $\sigma_{max} = 300$ MPa. The thickness of the metal plate is 1.2 mm. Spot welding was performed by Peugeot-Citroen-SA with its own welding parameters. The spotweld diameter is about 6 mm. The imposed velocity is taken in the quasi-static range ($V_{imp} = 2$ mm/min). Five tensile/shear ratio are chosen to characterise the spotweld behaviour ($\alpha = \{0°, 30°, 45°, 60°, 90°\}$). The failure patterns of the specimens are close to those given by Lin et al. (2002). Fig. 7 shows the cross-section of failed spotwelds. For pure opening loading conditions, the stresses are concentrating all around the welded point. Plasticity develops in this area and failure occurs by the through thickness shear in the heat affected zone (Fig. 7). This fracture mechanism is similar to pull-out tensile specimens. For combined and pure shear loading conditions, necking due to stretching appears in the base metal near the heat affected zone. The failure is initiated by necking/shear and propagates around the circumference of the welded point and in the metal plate. Finally, the metal plate is torn off (Fig. 7). This fracture mechanism is similar to single lap or coach-peel specimens. The experimental observations show that the failure of spotwelds involves crack initiation and growth under fully plastic conditions.

Lin et al. (2003) has developed a new general failure criterion (forces and moments) for spotwelds based on his new experimental database and the results from Lee et al. (1998). A simplified expression of this criterion is also proposed for pure and combined opening and shear loading (10). α parameter is equal to 1 for uniaxial opening loading conditions such as in Lee et al. (1998) specimen and to 0.5 for equal biaxial

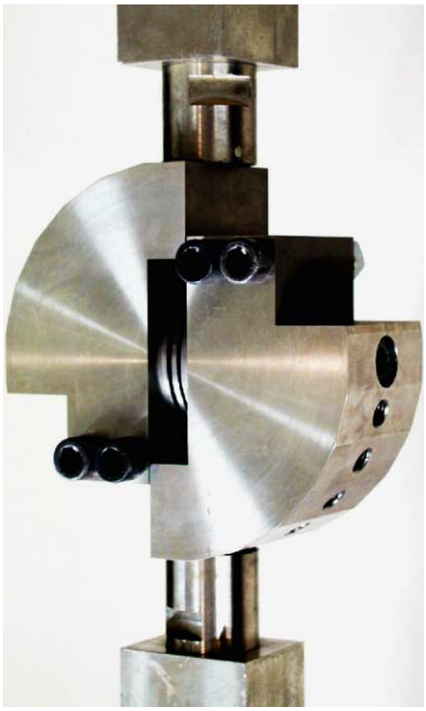

Fig. 6. Arcan type device.

opening loading conditions such as in Lin et al. (2002) specimen. For biaxial opening loading conditions, such as the author and Lin specimens, Lin et al. (2003) has shown that the maximum load in relation (8) is estimated from the maximum opening loads divided by $\sqrt{2}$.

$$[1-2\alpha+2\alpha^2]\overline{N}^2+\left[\frac{1}{3}+\left(\frac{4t}{\pi D}\right)^2\right](k\overline{T})^2=1 \tag{10}$$

where t is the sheet base material thickness, D is the spotweld diameter and k is the fitting constant of the criterion.

Normalized opening and shear loads (9) have then been derived from experimental results based on the maximum force in Eq. (8) (Table 1). Results show the influence of the specimen loading conditions (uniaxial or biaxial) when compared to Lee et al. (1998) and Lin et al. (2003) (Fig. 8). Authors results agree with Lin et al. (2003) experimental data obtained in biaxial loading conditions. The simplified failure criterion enables to model the pure opening and the mixed load conditions ($k = 1.25$). But as reported as Lin et al. (2003), the simplified failure criterion hardly succeeds in correlating experimental data in pure shear load conditions (Fig. 9). In that case, the failure is initiated in the heat-affected zone of the spotweld but the failure propagates in the base metal. To correlate pure shear experimental data, the fitting constant k (10) must be equal to 0.9 but the mixed load conditions are clearly underestimated (Fig. 9). The interest in the Arcan experimental set-up and results (and especially pure shear) is to improve the representativeness of criterion or to develop new model to better take into account the behaviour of the spotweld in pure shear.

Fig. 10 plots the load vs. displacement diagrams obtained for each tensile/shear ratio. These plots will be used for the optimisation of the previous joint element parameters.

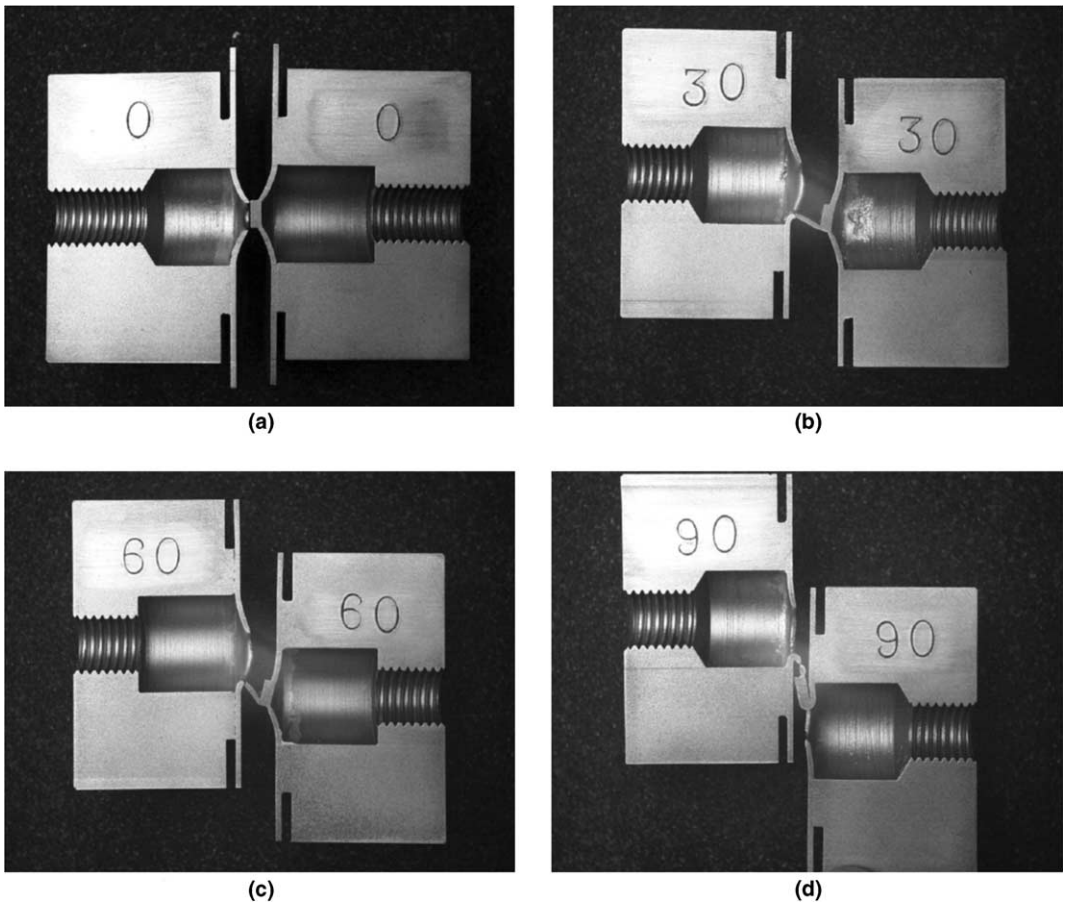

Fig. 7. Cross section of failed spotwelds: (a) $\alpha = 0°$, (b) $\alpha = 30°$, (c) $\alpha = 60°$, (d) $\alpha = 90°$.

Table 1
Normalized opening and shear local loads

Authors (th = 1.2 mm and $D = 6.0$ mm)			Lee et al. (1998) (th = 0.89 mm and $D = 6.4$ mm)			Lee et al. (1998) (th = 0.89 mm and $D = 4.3$ mm)			Lin et al. (2002) (th = 1.0 mm and $D = 6.4$ mm)			Lin et al. (2002) (th = 1.5 mm and $D = 6.4$ mm)		
α [°]	$\overline{N}$	$\overline{T}$	α [°]	$\overline{N}$	$\overline{T}$	α [°]	$\overline{N}$	$\overline{T}$	α [°]	$\overline{N}$	$\overline{T}$	α [°]	$\overline{N}$	$\overline{T}$
0	1.41	0.00	0	1.00	0.00	0	1.00	0.00	0	1.41	0.00	0	1.41	0.00
30	1.01	0.59	20	0.82	0.30	20	0.82	0.30	22	1.32	0.53	22	1.33	0.53
45	0.91	0.91	40	0.69	0.57	40	0.65	0.55	45	0.90	0.90	45	0.92	0.92
60	0.65	1.12	60	0.48	0.84	60	0.49	0.85	60	0.67	1.16	60	0.64	1.11
90	0.00	1.78	90	0.00	1.23	90	0.00	1.29	90	No data	No data	90	No data	No data

Experimental results are now given in terms of equivalent yield force F_y, and peak of loading F_m. Displacement measured at F_m is noted $\delta(F_m)$ and displacement at failure δ_u (Table 2). The total energy is noted E_t and energies absorbed before and after the peak of loading are noted E_1 and E_2 respectively. The analysis

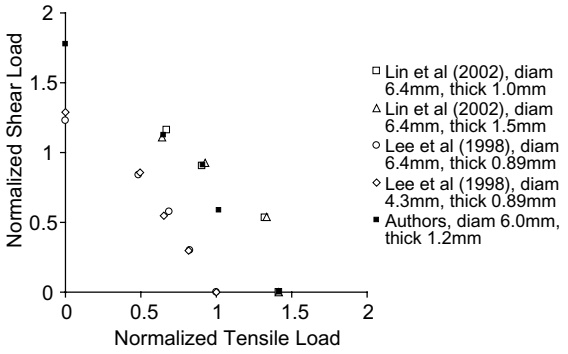

Fig. 8. Normalized failure criterion defined from Arcan type experiments and open literature.

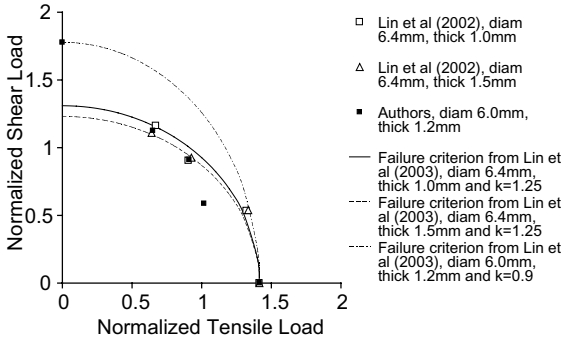

Fig. 9. Failure criterion from Lin et al. (2003).

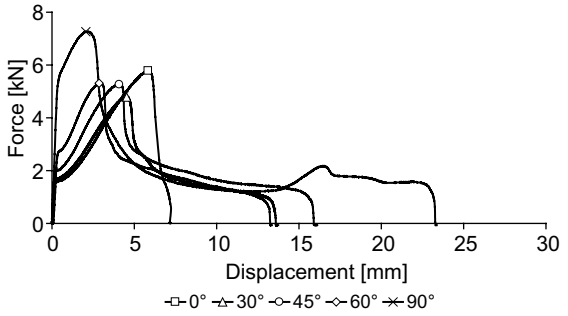

Fig. 10. Load vs. Displacement diagrams from Arcan type device.

shows that the regression for $F_y(\alpha)$ and $F_m(\alpha)$ is correct using a second-rate polynomial. For $\delta(F_m(\alpha))$, $\delta_u(\alpha)$ and $E(\alpha)$ the regression may be linear. In the case of a spotweld, the analysis of experimental results shows that the relations (6) or (10) cannot be used as a criterion at failure but as a threshold for damage processing. The energy absorbed after the peak of load by the spotweld is more and more important when the angular position goes to pure shear ($E_1(90°) \ll E_2(90°) \approx E_t(90°)$). To keep using that kind of criterion for failure and $F = F_m$, relations (6) or (10) should be connected to another criterion as the energy absorbed after the peak, E_2, as a function of the angular position α.

Table 2
Experimental data from Arcan type tests

α [°]	F_y [kN]	F_m [kN]	$\delta(F_m)$ [mm]	δ_u [mm]	E_1 [N mm]	E_2 [N mm]	E_t [N mm]
0	1.42	5.78	5.84	7.20	20 942	4 152	25 094
30	1.65	4.80	4.50	13.6	13 893	15 047	28 940
45	1.98	5.26	4.05	15.9	14 503	22 100	36 603
60	2.65	5.31	2.90	23.0	10 512	19 339	29 851
90	5.33	7.26	2.17	13.3	12 549	40 733	53 282

4. Identification of the joint model parameters

The new joint equivalent element uses an elastic–plastic model to describe the non-linear behaviour of the spotweld and a damage model to simulate its failure. The non-linear behaviour is given by the parameters: A, B and n (11). The parameters for the damage model are: D_c, P_s and P_u. Other parameters have been added to characterise shear and bending behaviours: A_y and A_z, and B_y and B_z, respectively. In first approximation, the model assumes: $A_y = A_z$ and $B_y = B_z$. The initial value of the parameters are: $A = 30$ MPa, $B = 1500$ MPa, $n = 0.9$, $A_y = B_y = 0.2$, $D_c = 0.8$, $P_s = 0.7$ and $P_u = 1.6$.

$$\sigma = A + B\varepsilon_p^n \tag{11}$$

The problem optimisation method consists in minimising the difference between experimental variables and those from the numerical model. The internally developed program (Langrand et al., 1999) is used to optimise the parameters of the model. This program is based on the conjugate gradient method and on the Davidon–Fletcher–Powell and Broyden–Fletcher–Goldfarb–Shanno (DFP and BFGS) algorithms (Polak, 1971). The criterion or cost function is defined by the least error squares method (12).

$$f(\underline{z}) = \sum_{N_p} \frac{(w_{num}(\underline{z}) - w_{exp})^2}{w_{exp}^2} \tag{12}$$

where N_p represents the number of experimental points, $\underline{z}$ is the parameter vector to be identified, w_{exp} and w_{num} are an experimental and a numerical measurement.

A sensitivity study has been performed first to rate the parameters and eventually in order to optimise only the necessary ones. The optimisation plan has been defined as follow:

(i) identification step 1: parameters A, B and n using the pure tensile Arcan type test,
(ii) identification step 2: parameters A_y, D_c, P_s and P_u using the pure shear Arcan type test.

The parameter B_y cannot be identified with the Arcan type test (no sensitivity) because the force does not generate moments in the joint model. The interest in the Arcan type tests is to enable parameter validation using mixed load tests.

Optimisation no. 1 leads to the following parameter values: $A = 1$ MPa, $B = 1650$ MPa and $n = 1$. The optimisation process has first decreased the value of the yield stress, A, and put the exponent, n, to its upper bound value. Then the optimisation process has fit the experimental curve using the parameter B (Fig. 11). Optimisations have been tried without upper bound for parameter n but numerical instabilities appeared. So it has been decided to keep the first solution, which is in a good agreement with the experiment, and to continue the optimisation process with the step 2.

Optimisation no. 2 leads to the following parameter values: $A_y = 0.3$, $D_c = 0.46$, $P_s = 0.01$ and $P_u = 1.82$. The force vs. displacement diagram is correctly described up to the maximum force even if the stiffness is lightly under estimated. Nevertheless, the joint model does not predict the energy absorbed after the load

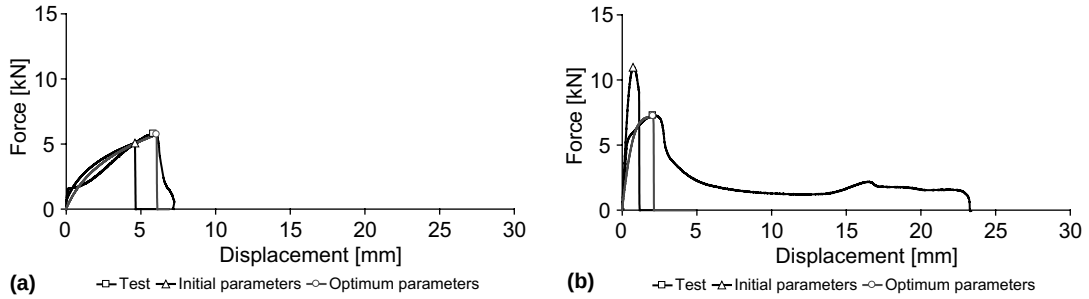

Fig. 11. Optimisation of equivalent joint model parameters: (a) no. 1: pure tension, (b) no. 2: pure shear.

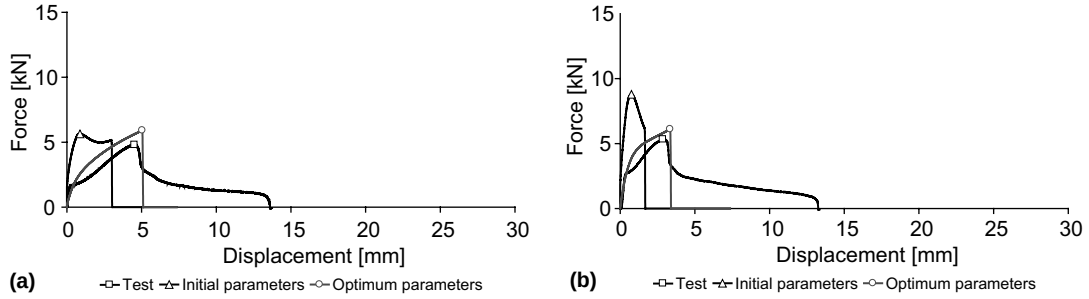

Fig. 12. Validation of the equivalent joint model parameters using mixed Arcan type tests: (a) $\alpha = 30°$, (b) $\alpha = 60°$.

peak (Fig. 12). For pure shear load, the energy available after the peak of load represents the most important part of the total energy. For crashworthiness the prediction of the energy absorbed in the joints may pilot strongly the structural kinematic. So there is a real interest in improving that part of the joint model.

The first step in the parameter validation process is to predict the response of Arcan type tests obtained for mixed loads. FE results are compared to experiment for angular positions $\alpha = 30°$ and $60°$ in Fig. 12. As for experiment, FE responses are presented in terms of F_m, $\delta(F_m)$ and E_1 (Table 3). The model predicts reasonably well the first part of the response of the weld but is unable to predict the post-peak response especially in the case of pure shear. The interest in the new joint model is to describe the elastic and plastic experimental behaviours for all tensile/shear ratios up to the maximum force. The energy at failure is underestimated for mixed opening and shear load and also for pure shear load.

The second step in the parameter validation process concerns the prediction of the mechanical behaviour of more standard samples such as the tensile pull-out, shear single lap or coach-peel specimens

Table 3
Analysis of Arcan type FE computations

α [°]	F_m [kN]	$\delta(F_m)$ [mm]	E_1 [N mm]	$\theta(F_m)$	$\theta(\delta(F_m))$	$\theta(E_1)$
0	5.73	6.05	22 514	0.01	0.04	0.08
30	5.90	5.05	20 393	0.23	0.12	0.47
45	5.95	4.17	17 860	0.13	0.03	0.23
60	6.10	3.35	15 598	0.15	0.15	0.48
90	7.20	2.08	11 678	0.01	0.04	0.07
			Mean value	0.10	0.07	0.25

Where $\theta(i) = \frac{|i^{exp} - i^{num}|}{i^{exp}}$.

(Figs. 13–15). Specimens are made of the same material. Welding is made with the same parameters (Peugeot-Citroen-SA) and the spotweld diameter is about 6 mm. The specimen width is about 40 mm. The length of specimens is: 125 mm for pull-out type, 2×85 mm for coach-peel type and 2×105 mm for shear single lap type. The clamping distance is about 40 mm. Five specimens are tested by Peugeot-Citroen-SA (Figs. 13–15) for each experimental configuration. The specimen width is split into five shell finite elements. The element length is adapted to keep shell shape as square as possible. Using that kind of mesh size, the computational time step is about $\Delta t = 1.6 \times 10^{-3}$ ms. The material behaviour is modelled with a Ludwik constitutive model (11) where parameters are: $A = 180$ MPa, $B = 300$ MPa and $n = 0.3$.

The non-linear behaviour of the specimen is not correctly predicted for the pull-out (Fig. 13) and shear single lap specimens (Fig. 14). Nevertheless, the distance between the experiment and the FEM remains correct (about 20% for the maximum load in the case of the pull-out specimen). For the coach-peel specimen, the non-linear behaviour of the FEM is in a good agreement compared to the experiments (Fig. 15). As reported in the Arcan type test, the failure part observed after the peak of load for both single lap and coach-peel specimens is not modelled by the computations. Other computations on pull-out, lap-shear and coach-peel specimens have shown that the non-linear behaviour of that kind of specimens depends on material and geometric parameters of the metal plate FE model. Indeed, out of plane deformations are very mesh dependant and the global response is also a function of the material parameters. Other parametric studies such as the influence of the joint element position within the connected shell element have been investigated. FE results show that small variations of this geometrical parameter may particularly modified

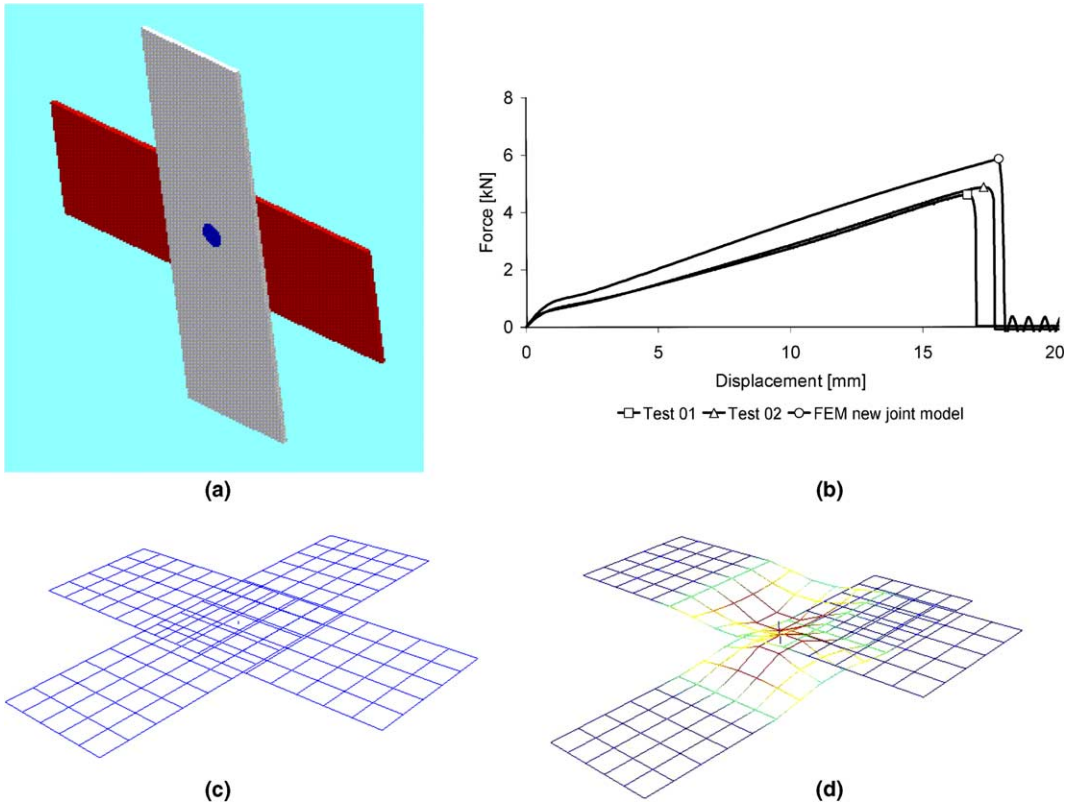

Fig. 13. Tensile pull-out test: (a) specimen, (b) comparison FEM/experiment, (c) undeformed FE mesh, (d) FE mesh before failure.

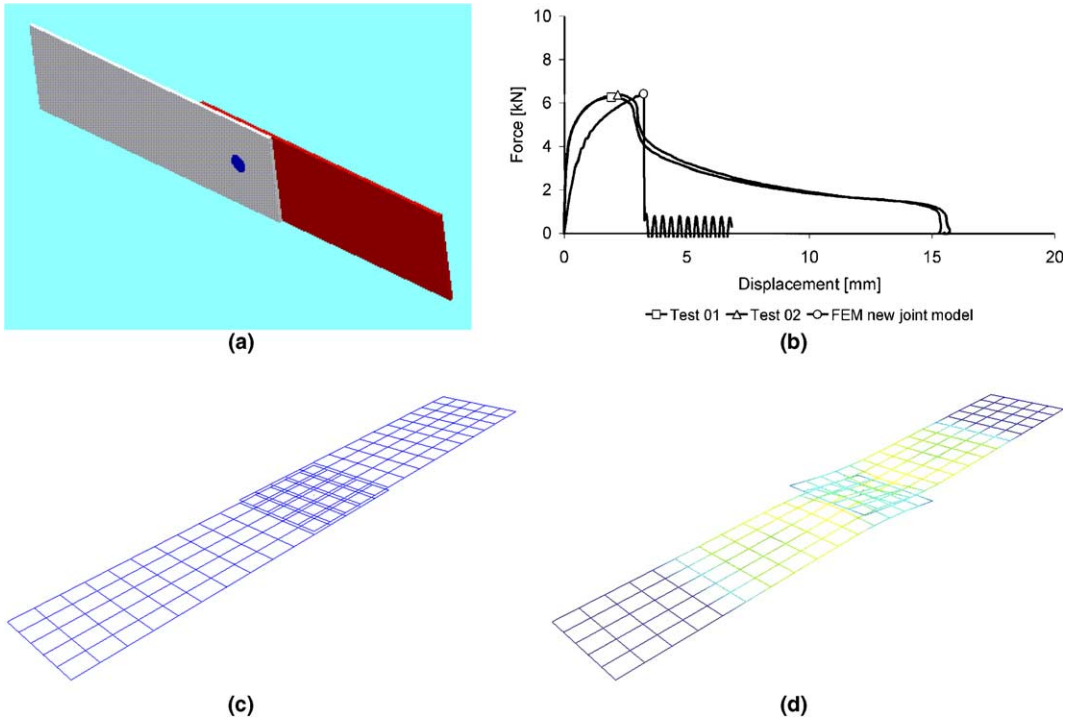

Fig. 14. Shear single lap test: (a) specimen, (b) comparison FEM/experiment, (c) undeformed FE mesh, (d) FE mesh before failure.

the global non-linear response of that kind of specimens. In our FE simulations, the joint element is supposed to be located exactly in the middle of the specimen width.

The new joint model has been also compared to a current method uses in structural calculations based on the use of a 6 DOF generalised spring. The mechanical properties of the spring are defined in pure tension and pure shear using Arcan type test and tabulated curves. The responses observed in Arcan mixed load cases have never been correctly predicted without tuning the spring inputs.

5. Conclusion

The paper deals with the implementation of a new joint equivalent model and experimental procedure for model characterisation. The first part presented a relatively simple model of the non-linear damage behaviour of a welded junction between two plates. The model simulates the global response of the weld and of a small portion of the welded plates. The second part of the paper concerned a new experimental procedure for joint model characterisation in pure and mixed tensile/shear loading. The experiments are based on Arcan principle. The parameters of the joint model are then identified using pure shear and pure tensile experimental results. The first step in the parameter validation step was to simulate mixed tensile/shear experiments. The model has predicted reasonably well the first part of the response of the weld but is unable to predict the post-peak response especially in the case of pure shear. The second step in the parameter validation process has concerned the prediction of the mechanical behaviour of more standard samples such as the tensile pull-out, shear single lap or coach-peel specimens. The FE model has succeeded in predicting reasonably the global responses of those kinds of samples.

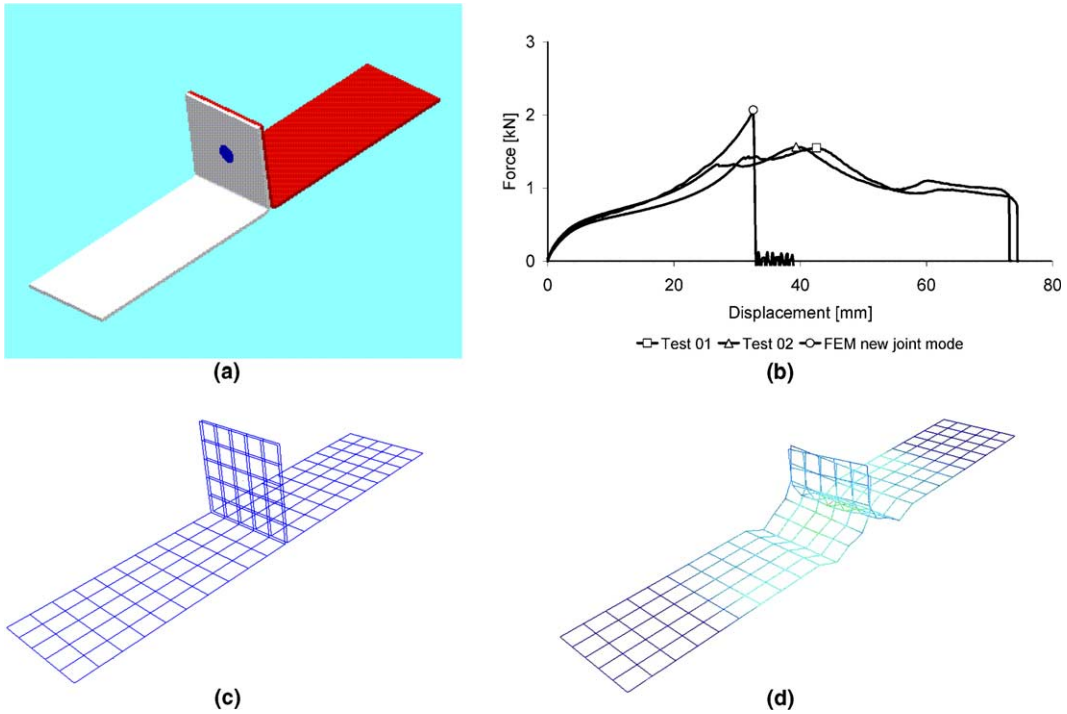

Fig. 15. Coach-peel test: (a) specimen, (b) comparison FEM/experiment, (c) undeformed FE mesh, (d) FE mesh before failure.

Finally, the results have shown the capability of the Arcan type test to characterise the experimental non-linear behaviour of the spotwelds and the parameters of joint equivalent models. The interest in such an experimental device is also to assess the representativeness of failure criterion and the capability of joint equivalent model used in crashworthiness analysis. Regarding the use of the presented joint model for spotweld, results have shown that the element fails in describing the behaviour of the joint observed after the peak of load. New developments will concern improvements in the modelling of the failure and could be based on the energy E_2, which has been characterised with the Arcan type device.

Only static loads have been investigated in the present work. Future works will concern dynamic aspects, which are prime of interest for structural crashworthiness. The strain rate dependency of the spotweld response will be studied using specific Arcan type tests in order to improve the joint equivalent model if necessary.

Acknowledgements

The authors thank the French ministry of industry, which partially supported this research program under the PREDIT research program Grant no PREDIT 98 A0149.

References

Arcan, M., Hashin, Z., Voloshin, A., 1978. A method to produce uniform plane-stress states with applications to fiber-reinforced materials. Exp. Mech. 35, 141–146.

Belytschko, T., Tsai, C., 1983. A stabilization procedure for quadrilateral plate element with one point quadrature. Int. J. Num. Meth. Eng. 19, 405–419.

Chapuliot, S., Combescure, A., 1993. Flambage plastique des coques cylindriques raidies axialement. Revue Européenne des Éléments Finis 2, 449–464.

Combescure, A., Delcroix, F., Caplain, L., Espanol, S., Eliot, P., 2003. A finite element to simulate the failure of weld point on impact. Int. J. Impact Eng. 28, 783–802.

d'Almeida, J.R.M., Monteiro, S.N., 1999. The Iosipescu test method as a method to evaluate the tensile strength of brittle materials. Polymer Testing 18, 407–414.

Dvorkin, E., Bathe, K.J., 1984. A continuum mechanics four nodes shell element for general non linear analysis. Eng. Comput. 1, 77–88.

Hanseen, A.G., Langseth, M., 2003. Identification and modelling of self-pierce rivet failure for crash analyses. In: Proceeding of MecaMat Conf., Aussois, France.

Illyushin, A., 1956. Plasticité. Eyrolles, Paris, France.

Iosipescu, N., 1967. New accurate procedure for single shear testing of metals. J. Mater. 2 (3), 537–566.

Langrand, B., Fabis, J., 2002. Dynamic effects on riveted joints using Arcan test procedure. EU Programme Crashworthiness of Aircraft for High Velocity Impact (G4RD-CT-2000-00395), Deliverable no D.5.1.2.

Langrand, B., Geoffroy, P., Petitniot, J.L., et al, 1999. Identification technique of constitutive model parameters for crashworthiness modelling. Aerospace Sci. Technol. 3 (4), 215–227.

Langrand, B., Deletombe, E., Markiewicz, E., Drazétic, P., 2000. Characterisation of dynamic failure for riveted joint assemblies. Shocks Vib. 7 (3), 121–138.

Langrand, B., Deletombe, E., Markiewicz, E., Drazétic, P., 2001. Riveted joint modelling for numerical analysis of airframe crashworthiness. Finite Element Anal. Des. 38 (1), 21–44.

Lee, Y.L., Wehner, T.J., Lu, M.W., Morrissett, T.W., Pakalnins, E., 1998. Ultimate strength of resistance spot welds subjected to combined tension and shear. J. Testing Eval. 26 (3), 213–219.

Lemaitre, J., Chaboche, J.L., 1985. Mécanique des matériaux solides. Bordas, Paris, France.

Lin, S.H., Pan, J., Wu, S.R., Tyan, T., Wung, P., 2002. Failure loads of spot welds under combined opening and shear static loading conditions. Int. J. Solids Struct. 39, 19–39.

Lin, S.H., Pan, J., Tyan, T., Prasad, P., 2003. A general failure criterion for spot welds under combined loading conditions. Int. J. Solids Struct. 40, 5539–5564.

Markiewicz, E., Ducrocq, P., Drazétic, P., Haugou, G., Fourmentraux, T., Bérard, J.Y., 2001. Material behaviour law identification for the various zones of the spot-weld under quasi-static loadings. Int. J. Mater. Product Technol. 16 (6–7), 484–509.

Patronelli, L., Langrand, B., Deletombe, E., Markiewicz, E., Drazétic, P., 1999. Analysis of riveted joint failure under mixed mode loading. Eur. J. Mech. Environ. Eng. 44 (4), 223–228.

Polak, E., 1971. Computational Methods in Optimisation. In: Mathematics in Sciences and Engineering 77. Academic Press.

RADIOSS CRASH, 1998. Guidelines and user's manual. Version 4.1. MECALOG, 06903 Sophia Antipolis Cedex France.

Riesner, M., Sun, X., Wu, S., et al., 2000. Modelling and optimisation of structural joints in automotive applications. In: Proceeding of the 2nd Int. Crashworthiness Conf. The Royal Aeronautical Society, London.

Sutton, M.A., Deng, X., Ma, F., Newman, J.C., James, M., 2000a. Development and application of a crack Tipp opening displacement-based mixed mode fracture criterion. Int. J. Solids Struct. 37, 3591–3618.

Sutton, M.A., Boone, M.L., Ma, F., Helm, D., 2000b. A combined modelling-experimental study of the crack opening displacement fracture criterion for characterisation of stable crack growth under mixed mode I/II loading in thin sheet materials. Eng. Fract. Mech. 66, 171–185.

Voloshin, A., Arcan, M., 1980. Failure of unidirectional fiber-reinforced materials—new methodology and results. Exp. Mech. 37, 280–284.

Wang, D.A., Lin, S.H, Pan, J., 2004. Stress intensity factors for spot welds and associated kinked cracks in cup specimens. Int. J. Fatigue, submitted for publication.

Zeng, Q., Combescure, A., 1998. A new one point quadrature, general nonlinear quadrilateral shell element with physical stabilisation. Int. J. Num. Meth. Eng. 42, 1307–1338.